Journal of Cellular Biochemistry 63:23–36 (1996)

ARTICLES

Separate Analysis of Nuclear and Cytosolic Ca^{2+} Concentrations in Human Umbilical Vein Endothelial Cells

Masataka Ikeda, Hideo Ariyoshi, Jun-ichi Kambayashi, Kazumasa Fujitani, Nobutoshi Shinoki, Masato Sakon, Tomio Kawasaki, and Morito Monden

Department of Surgery II, Osaka University Medical School, 2-2 Yamadaoka, Suita, Osaka 565, Japan

Abstract Ca^{2+} concentration inside human umbilical vein endothelial cells was studied separately in cytosol and nucleus by a confocal laser scanning microscopy using fluo-3. The in vivo calibration curve for cytosol and nucleus showed good linearity between fluorescence intensity and Ca^{2+} concentration in cytosol ($[Ca^{2+}]_i$) and nuclei ($[Ca^{2+}]_n$). After calibration, $[Ca^{2+}]_n$ was constantly higher than $[Ca^{2+}]_i$ before and after the chelation of extracellular Ca^{2+} suggesting an active Ca^{2+} accumulation system on nuclear membrane. $[Ca^{2+}]_n$ was also constantly higher than $[Ca^{2+}]_i$ after the stimulation of thrombin (0.05 U/ml), FCS (10%), and thapsigargin (Tsg, 1 μM). The temporal change of $[Ca^{2+}]_n$ and $[Ca^{2+}]_i$ was identical, and $[Ca^{2+}]_i$ gradient towards the nucleus and peripheral or central $[Ca^{2+}]_n$ rise was observed after these stimulations. From these results, $[Ca^{2+}]_n$ is not only regulated by the active Ca^{2+} accumulation system on nuclear membrane at rest but also the generation of inositol-triphosphate. FCS caused heterogeneous $[Ca^{2+}]_n$ or $[Ca^{2+}]_i$ rise from cell to cell; single spike or oscillatory change of $[Ca^{2+}]_n$ and $[Ca^{2+}]_i$ was observed in about 56% of cells, which were completely abolished by the chelation of extracellular Ca^{2+}, suggesting that FCS stimulated $[Ca^{2+}]_n$ and $[Ca^{2+}]_i$ rise solely depending on Ca^{2+} influx from extracellular medium. The higher concentration of $[Ca^{2+}]_n$ and heterogeneous $[Ca^{2+}]_n$ rise may have important roles in nuclear-specific cellular responses. © 1996 Wiley-Liss, Inc.

Key words: $[Ca^{2+}]_i$ and $[Ca^{2+}]_n$, Ca^{2+} gradients, confocal laser scanning microscopy, Fluo-3, heterogeneity

The vascular endothelial cells (ECs) covering the luminal surface of vessel walls play an important role as a thromboresistent factor through the secretion or expression of anticoagulant factors [Person, 1993] and as a regulator of the smooth muscle tone via associated vasoactive substances [Rubanyi, 1993]. It is well known that several stimulations such as shear stress [Buga et al., 1991], hypoxia [Gertler et al., 1993], and hormonal stimuli including thrombin or other growth factors [Laposata et al., 1983] alter cell shape and affect various functions of ECs, in association with a rise in the cytoplasmic ionized calcium concentration ($[Ca^{2+}]_i$) [Himmel et al., 1993]. $[Ca^{2+}]_i$ or the ionized Ca^{2+} concentration of nuclei ($[Ca^{2+}]_n$) is believed to control many cellular functions, such as cell motility [Nicotera et al., 1990], secretion [Rasmussen, 1986], cell differentiation [Gillo et al., 1993], and the cell cycle [Poenie et al., 1985]. Recently $[Ca^{2+}]_n$ has been focused on because there exists the possibility that agonists transfer calcium signals not only to the cytosol but also to the nucleus [Nicotera et al., 1989; Burgoyne et al., 1989]. This possibility was further supported by the spatio-temporal analysis of $[Ca^{2+}]_i$ or $[Ca^{2+}]_n$ employing digital imaging fluorescent microscopic systems. The Ca^{2+} gradient between cytosol and nucleus at rest and under stimulations has been demonstrated using digital imaging microscopy with the fluorescent Ca^{2+}-indicator, fura-2 [Williams et al., 1985; Wahl et al., 1992; Geiger et al., 1992; Goldman et al., 1990; Tucker and Fay, 1990; Yelamarty et al., 1990]. As the fura-2 ratio in the nucleus and the cytosol was diverse even at rest, the implications of the results have remained controversial, partly because of the limitations in the systems, and the differences of the dye characteristics in the nucleus and the cytosol, and in the cell types. The limitations include the artifacts due to ratioing of fura-2 fluorescence [Moore et al., 1990]. Since it takes at least a few seconds to

Received January 19, 1996; accepted March 28, 1996.

Address reprint requests to Masataka Ikeda, M.D., Department of Surgery II, Osaka University Medical School, 2-2 Yamadaoka, Suita, Osaka 565, Japan.

© 1996 Wiley-Liss, Inc.

acquire each F340, F380, or background image when employing distributed imaging system, the calculated ratio image does not reflect the actual $[Ca^{2+}]_i$ or $[Ca^{2+}]_n$ distribution if each image is not properly overlapped. Moreover, fluorescence images of fura-2 include the images of the focused plane as well as out-of-focus planes, which makes it difficult to distinguish fluorescence of the nucleus from that of cytosol. Even with controlled illumination, the fluorescence of fura-2 tends to become bleached out after prolonged illumination due to UV excitation, which also causes artifacts by affecting the signal-to-noise ratio. In order to avoid these artifacts due to fura-2 ratioing technique, a confocal laser scanning microscopy (CLSM) with the visible light excitable dye fluo-3, more resistant to photo-bleaching and giving better resolution [Minta et al., 1989], has been employed [Kuba et al., 1991; Hernandez-Cruz et al., 1990; Nakato et al., 1992; Burnier et al., 1994]. Although Kuba et al. [1991] did not observe apparent rise in $[Ca^{2+}]_n$ stimulated by either depolarization or caffeine, Hernandez-Cruz et al. [1990], Nakato et al. [1992], and Burnier et al. [1994] demonstrated the higher fluorescence intensity in nuclear region in voltage-clamped vertebrate neuron, in basophilic leukemia cells stimulated with antigen and in cultured vascular cells stimulated with angiotensin II or vasopressin, respectively. But the physiological implications of higher fluorescence intensities inside nucleus have been controversial. Burnier et al. [1994] demonstrated that the calibrated $[Ca^{2+}]_n$ was lower than the calibrated $[Ca^{2+}]_i$ at rest and that calibrated $[Ca^{2+}]_n$ and $[Ca^{2+}]_i$ were similar after stimulation, inconsistent with the results of shear stressed ECs observed by Geiger et al. [1992]. We therefore conducted this study to elucidate the relationship between $[Ca^{2+}]_i$ and $[Ca^{2+}]_n$ at rest and under stimulation spatio-temporally using thrombin and FCS, known agonists for ECs and thapsigargin, Ca^{2+}-ATPase inhibitor. Thrombin is a key regulatory protein of thrombosis and hemostasis, and recent studies using fluorescent Ca^{2+} indicators have shown that thrombin causes rapid $[Ca^{2+}]_i$ rise in bovine pulmonary artery endothelial cells [Goligotsky et al., 1989] and in HUVECs [Hallam et al., 1988; Lerner, 1994]. Thrombin-induced $[Ca^{2+}]_i$ rise is composed of an initial $[Ca^{2+}]_i$ peak and a sustained phase. The former is mainly dependent on the Ca^{2+} release from internal storage sites induced by inositol-triphosphate (IP_3), and the latter is dependent on Ca^{2+} influx across the plasma membrane. Thapsigargin has been shown to inhibit the endoplasmic reticular Ca^{2+}-ATPase and has been used to investigate the signal transduction mechanism of $[Ca^{2+}]_i$ [Thastrup et al., 1990; Lytton et al., 1991; Haller et al., 1994; Gericke et al., 1994]. In vivo calibration curves for the nuclei and cytosol were first established, which were not demonstrated in the previous reports employing CLSM and fluo-3 [Kuba et al., 1991; Hernandez-Cruz et al., 1990; Nakato et al., 1992; Burnier et al., 1994], and then we could clearly demonstrate the $[Ca^{2+}]_n$ and $[Ca^{2+}]_i$ change in stimulated HUVECs by thrombin, thapsigargin (Tsg), or FCS.

MATERIALS AND METHODS

Materials

Fluo-3 acetoxymethyl ester (AM) was obtained from Molecular Probes (Eugene, OR), fetal calf serum (FCS) from JRH Biosciences (Lenexa, KS), and MCDB131 culture medium from Chlorella Inc. (Tokyo, Japan). Recombinant human b-FGF was obtained from DaiNippon Pharmaceutical Inc. (Osaka, Japan). Cremophor EL, detergent was from nacalai tesque (Kyoto, Japan). Penicillin-streptomycin from Life Technologies, Inc. (Grand Island, NY), thapsigargin from Sigma Chemical Company (St. Louis, MO), and digitonin from Wako Pure Chemical Industries (Osaka, Japan) were used. α-thrombin was kindly donated by Mochida Pharmaceutical Co. Ltd. (Tokyo, Japan). Other chemicals were of the highest analytical grade available.

Cell Culture and Dye Loading

Human umbilical vein endothelial cells (HUVECs) were obtained from human umbilical veins primarily by the methods described by Jaffe et al. [1973] with some modifications. HUVECs were characterized as ECs by their typical cobblestone appearance and the positive staining for VIII antigen. Passage of cells was performed as soon as the monolayers reached confluence. Cells were grown in monolayers in medium containing MCDB131, penicillin (100 U/ml)-streptomycin (100 μg/ml), basic-FGF (10 ng/ml), and 10% FCS. Cells coming from one single cord before the 9th passage were used for Ca^{2+} measurement and were subcultivated on cover slips placed on the bottom of a Flexiperm chamber (Heraeus Biotechnologie, Hanau, Ger-

many) 2 days before the experiments. Cell synchronization at the G0 stage was carried out by fasting HUVECs without FCS for 24 h. Ca^{2+} indicator, fluo-3 [Minta et al., 1989], loading was performed by incubating cells in modified Hepes Tyrode's buffer (129 mM NaCl, 8.9 mM $NaHCO_3$, 0.3 mM KH_2PO_4, 0.8 mM $MgCl_2$, 5.6 mM dextrose, and 10 mM Hepes, pH 7.4) containing 10 μM fluo-3/AM for 45 min at 37°C in the presence of 0.02% Cremophor EL. Cells were washed twice with modified Hepes Tyrode's buffer and mounted on a Zeiss Axiovert 135 inverted microscope at room temperature (Carl Zeiss, Microscope Division, Oberkochen, Germany). All experiments were performed for less than 90 min after dye loading.

$[Ca^{2+}]_i$ and $[Ca^{2+}]_n$ Imaging

Digital imaging was carried out as described previously [Burnier et al., 1994] with some modifications. A CLSM equipped with an argon-ion laser (Carl Zeiss Microscope Systems LSM 410, Oberkochen, Germany) was employed in this study. A 488 nm laser light was used for excitation; emitted light was collected through a FT510 dichroic beam splitter and finally passed through a 515 nm long pass filter. A 40 × oil-immersion objective (Plan-neofluar, numerical aperture = 1.3) was used. As the focal depth of the optical section can be controlled by varying the size of the aperture pinhole in the emission pathway, we adjusted the size of the aperture pinhole to obtain the focal depth of approximately 0.6 μm, which is sufficiently small to obtain the fluorescence intensity independently of the thickness of the specimen. We focused on the focal plane including the nucleus and the cytoplasm by z-sectioning. Artifacts due to photobleaching during temporal examination were minimal (more than 98% of the initial fluorescence in each preparation still remained after 13 min laser exposure). Images acquired by a photo multiplier tube (PMT) detector were averaged in real time to reduce noise, and the average was digitized to 256 gray levels with an analog-to-digital converter. Images of 512 × 512 pixels were employed.

Determination of $[Ca^{2+}]_i$ and $[Ca^{2+}]_n$

In the examination of the sensitivity and the linearity of the system for the concentration of ionized Ca^{2+} inside HUVECs, in vivo calibration curves for fluo-3 fluorescence were made separately for cytosol and nuclei by addition of 25 μM digitonin in various concentrations of extracellular Ca^{2+} adjusted with Ca^{2+}/ethylene glycol bis(β-aminoethyl ether)-*N*,*N*,*N*′,*N*′-tetraacetic acid (EGTA) buffer [Harafuji and Ogawa, 1980] at room temperature. The mean fluorescence intensity of individual cells was calculated as the average of fluo-3 fluorescence intensity in each pixel for the cytosol or nuclei after the fluorescence intensity reached equilibrium, which was achieved by 25 μM digitonin treatment. Although digitonin has no selectivity and increases plasma membrane permeability of fluo-3 as well as Ca^{2+}, we could obtain Ca^{2+} equilibrium before fluo-3 leakage with 25 μM digitonin treatment. Nucleus and cytosol were identified by differential interference contrast images taken before obtaining fluo-3 images. As shown in Figure 1, the fluorescence intensity of fluo-3 from cytosol and nuclei increased linearly as the concentration of extracellular Ca^{2+} increased

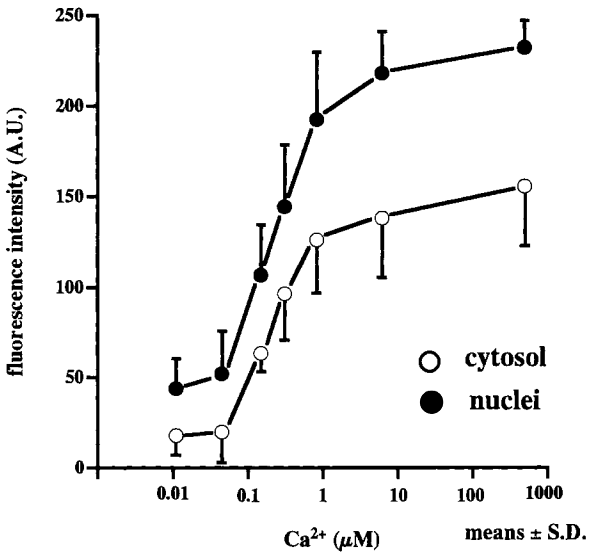

Fig. 1. In vivo calibration curves in cytosol and nuclei. Fluo-3 loaded human umbilical vein endothelial cells (HUVECs) were prepared by incubating cells with 10 μM fluo-3/AM at 37°C for 45 min. After washing away of unloaded dye, the cells were incubated with 25 μM digitonin in the presence of extracellular Ca^{2+} at various concentrations adjusted by Ca^{2+}/EGTA buffer at room temperature. After the plateau was observed, 535 nm emission fluorescent images after excitation at 488 nm were obtained using the confocal laser scanning microscopic system as described in Materials and Methods. The mean value of fluorescence intensity in each pixel inside the cytosol or nuclear portion was calculated from acquired images. Nucleus and cytosol were identified by diffusion interference contrast images taken before obtaining fluo-3 images. The mean ± S.D. for data calculated from at least 7 cells is shown. The results shown are a typical representative of 3 different preparations.

TABLE I. Effect of EGTA on Changes in Cytosolic and Nuclear Calcium Concentrations in HUVECs Loaded with Fluo-3†

	Cytosolic			Nuclear		
	Baseline	8 min after	n	Baseline	8 min after	n
Control	83.7 ± 8.5	85.1 ± 14.8	14	176.9 ± 13.2	165.6 ± 14.5	15
EGTA	95.6 ± 6.3	27.5 ± 5.6*	11	194.2 ± 21.2	57.8 ± 5.6*	14

†Values are expressed as means ± sem in nM. Control: add buffer instead of EGTA.
*$P < 0.0001$ vs. baseline.

from 45 nM to 1 μM. This result demonstrated that the observed fluorescence intensity in cytosol and nucleus under physiological condition was proportional to the ionized Ca^{2+} concentration inside the focal plane, and fluorescence intensity in nucleus was stronger than that in cytosol at the same Ca^{2+} concentration. In each experiment, calibration of $[Ca^{2+}]_i$ or $[Ca^{2+}]_n$, was carried out by the method described by Gillo et al. [1993]. Briefly, at the end of each experiment, 25 μM digitonin was added to obtain maximal fluorescence (Fmax) followed by the addition of 10 mM EGTA to obtain minimal fluorescence (Fmin) and then we calculated the $[Ca^{2+}]_i$ or $[Ca^{2+}]_n$ value by averaging the fluorescence intensity (F), Fmax, and Fmin for the corresponding region of the given cell using the equation $[Ca^{2+}]_i$ or $[Ca^{2+}]_n = Kd \times (F - Fmin)/(Fmax - F)$, where Kd is the dissociation constant for Ca^{2+}-bound fluo-3 at 320 nM. When morphological change of the cell was noted by digitonin treatment, it was excluded for calibration.

Calculations and Statistics

Results are expressed as mean ± SE or SD when indicated. Comparisons between groups were performed using a Student's paired *t*-test. A *P* value of less than 0.05 was accepted as significant.

RESULTS

Effects of Extracellular Ca^{2+} on Temporal Changes and Spatial Distribution of $[Ca^{2+}]_i$ or $[Ca^{2+}]_n$

Without stimulation, the mean value of $[Ca^{2+}]_i$ or $[Ca^{2+}]_n$ in each single cell was heterogeneous from cell to cell and the mean value of $[Ca^{2+}]_n$ was significantly higher than that of $[Ca^{2+}]_i$ in the presence or absence of extracellular Ca^{2+} (Table I). As shown in Figure 2A, the chelation of extracellular Ca^{2+} by EGTA rapidly decreased both $[Ca^{2+}]_i$ and $[Ca^{2+}]_n$ in parallel in 3 min. In the presence of extracellular Ca^{2+}, the spatial distribution of $[Ca^{2+}]_i$ was inhomogeneous and $[Ca^{2+}]_i$ was highest around the nucleus (Fig. 2B-a), and several high Ca^{2+} spots were sometimes observed at this site (see arrows in Figs. 3C-a, 5C-a). These high Ca^{2+} spots around the nucleus were observed even after the chelation of extracellular Ca^{2+} (arrows Fig. 3C-d) suggesting that these high Ca^{2+} spots might be compartmentalizations into internal organelles as has been reported in previous reports where fluo-3 loading was carried out with membrane-permeant esters [Kuba et al., 1991; Kao et al., 1989]. The spatial distribution of $[Ca^{2+}]_n$ was almost homogeneous before and after the chelation of extracellular Ca^{2+}.

Effects of Thrombin on $[Ca^{2+}]_i$ or $[Ca^{2+}]_n$

In the presence of extracellular Ca^{2+}, thrombin (0.05 U/ml) caused heterogeneous transient rise in $[Ca^{2+}]_i$ and $[Ca^{2+}]_n$ which was followed by sustained elevation (△,▲), oscillatory spikes (○,●), or rapid decline (□,■) in $[Ca^{2+}]_i$ or $[Ca^{2+}]_n$ and the temporal changes of $[Ca^{2+}]_i$ and $[Ca^{2+}]_n$ were identical (Fig. 3A-a). As shown in Figure 3A-b, $[Ca^{2+}]_i$ and $[Ca^{2+}]_n$ rise rapidly declined to the basal level in the absence of extracellular Ca^{2+} and the temporal changes of $[Ca^{2+}]_i$ and $[Ca^{2+}]_n$ were also identical. As shown in Figure 3B and Table II, the mean peak $[Ca^{2+}]_i$ and $[Ca^{2+}]_n$ values at the initial spike in the presence of extracellular Ca^{2+} were comparable with those in the absence of extracellular Ca^{2+}, and sustained $[Ca^{2+}]_i$ and $[Ca^{2+}]_n$ rise were abolished by chelating extracellular Ca^{2+}, suggesting that the main source of Ca^{2+} elevating $[Ca^{2+}]_i$ and $[Ca^{2+}]_n$ at the initial spikes are the internal Ca^{2+} storage sites, and transmembrane Ca^{2+}

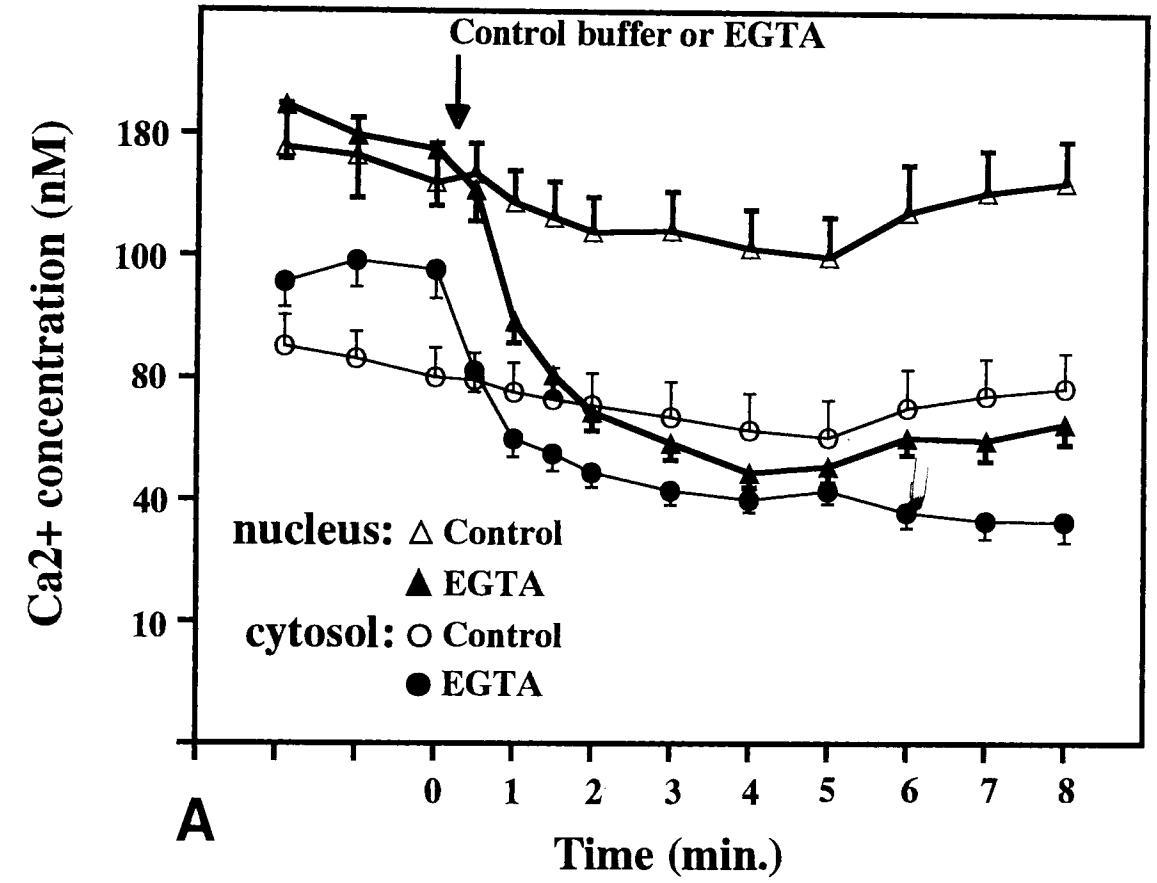

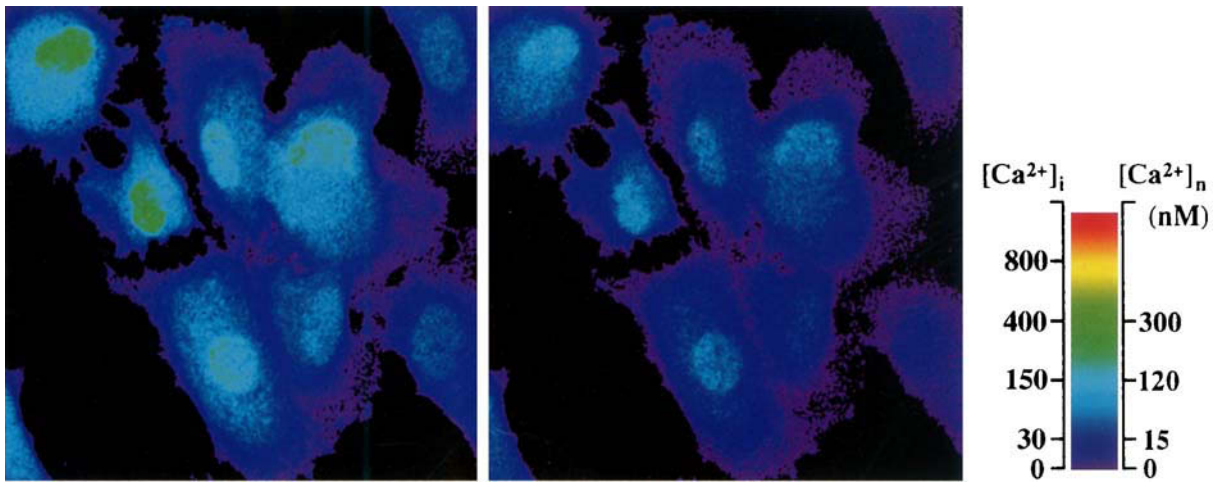

Fig. 2. **A:** Temporal changes of mean $[Ca^{2+}]_n$ and $[Ca^{2+}]_i$ value in HUVECs incubated in the presence of 1 mM $CaCl_2$ or absence of extracellular Ca^{2+}. **B:** Spatial distribution of ionized free Ca^{2+} inside HUVECs before (a) and after (b) the addition of EGTA to the extracellular medium. After 2-min incubation of fluo-3 loaded HUVECs in the presence of 1 mM extracellular Ca^{2+}, 2 mM of EGTA or control buffer was added at the time indicated by the arrow in A. Digital imaging was carried out every 6 s as described in Materials and Methods. Temporal changes of the mean $[Ca^{2+}]_n$ (△,▲) and $[Ca^{2+}]_i$ (○,●) value (A) and typical fields before (a) and 8 min after (b) the addition of EGTA into the extracellular medium are shown (B). The results presented here are typical representatives of 3 different preparations. Bar, 50 μm.

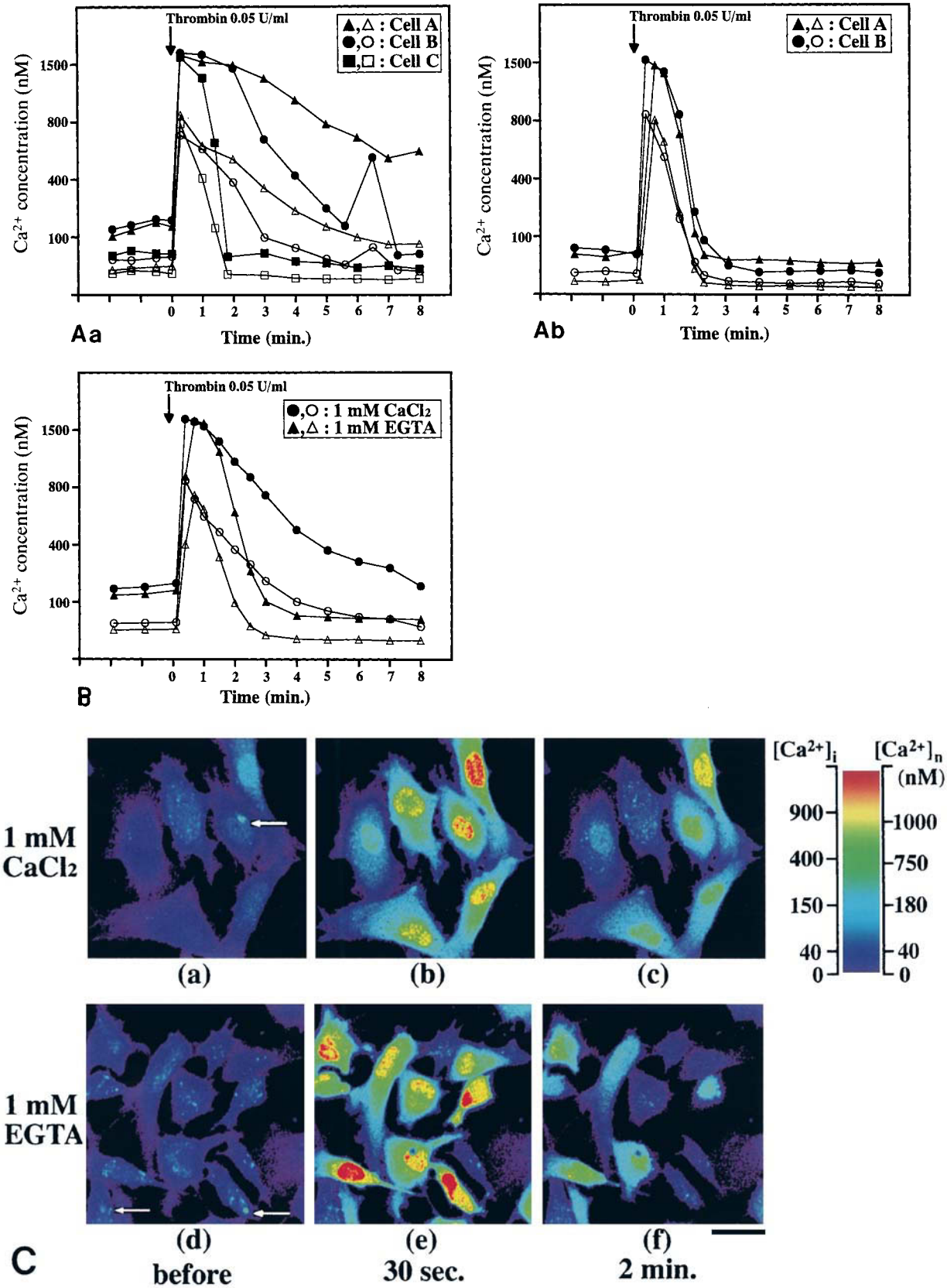
Thrombin 0.05 U/ml
▲,△ : Cell A
●,○ : Cell B
■,□ : Cell C
Ca2+ concentration (nM)
1500
800
400
100
0 1 2 3 4 5 6 7 8
Time (min.)
Aa
Thrombin 0.05 U/ml
▲,△ : Cell A
●,○ : Cell B
Ab
●,○ : 1 mM CaCl2
▲,△ : 1 mM EGTA
B
1 mM CaCl2
(a)
(b)
(c)
[Ca2+]i
[Ca2+]n
(nM)
900
400
150
40
0
1000
750
180
40
0
1 mM EGTA
(d) before
(e) 30 sec.
(f) 2 min.
C

Figure 3.

TABLE II. Effect of Thrombin (0.05 U/ml) on Changes in Cytostolic and Nuclear Calcium Concentrations in HUVECs Loaded with Fluo-3 in the Presence of 1 mM Extracellular Ca^{2+} or 1 mM EGTA†

	Cytosolic			Nuclear		
	Baseline	Peak	n	Baseline	Peak	n
1 mM Ca^{2+}	71.8 ± 5.6	1,099.0 ± 85.3*	40	105.4 ± 9.9	1,615.5 ± 19.2*	22
1 mM EGTA	46.4 ± 7.3	1,041.8 ± 129.4*	16	85.5 ± 13.3	1,562.4 ± 44.8*	16

†Thrombin was added 5 min after the addition of EGTA into the extracellular medium. Values are expressed as means ± sem in nM.
*$P < 0.0001$ vs. baseline.

influx is necessary for maintaining sustained elevation in $[Ca^{2+}]_i$ and $[Ca^{2+}]_n$. Since the temporal change in $[Ca^{2+}]_i$ was also heterogeneous from cell to cell in synchronized cells (data not shown), the observed heterogeneity in $[Ca^{2+}]_i$ or $[Ca^{2+}]_n$ transients was not due to cell cycle.

Figure 3C shows the spatial distribution of ionized Ca^{2+} in HUVECs before and after the stimulation by thrombin in the presence or absence of extracellular Ca^{2+}. Thirty seconds after the stimulation, $[Ca^{2+}]_i$ gradient towards the nucleus was observed in the presence or absence of extracellular Ca^{2+}. Although the spatial distribution of Ca^{2+} inside nucleus before stimulation was homogeneous, peripheral $[Ca^{2+}]_n$ rise or central $[Ca^{2+}]_n$ rise was observed after the stimulation in the presence or absence of extracellular Ca^{2+}.

Effect of FCS on $[Ca^{2+}]_i$ or $[Ca^{2+}]_n$ in HUVECs

Since FCS is known to stimulate cell proliferation and $[Ca^{2+}]_i$ rise [Gonzalez et al., 1988; Moolenaar et al., 1984; Wahl et al., 1990], we also tested the effect of FCS on both $[Ca^{2+}]_i$ or $[Ca^{2+}]_n$ in HUVECs synchronized to the G0 stage. Before stimulation, the mean value of $[Ca^{2+}]_i$ or $[Ca^{2+}]_n$ was 109.9 ± 8.6 nM or 198.7 ± 16.3 nM (n = 24), respectively. The response in $[Ca^{2+}]_i$ or $[Ca^{2+}]_n$ induced by 10% FCS was heterogeneous from cell to cell, but the temporal changes of $[Ca^{2+}]_i$ and $[Ca^{2+}]_n$ were identical (Fig. 4A and B). About a quarter (26%) of the cells (n = 27) showed transient $[Ca^{2+}]_i$ or $[Ca^{2+}]_n$ rise (Fig. 4B-a), a proportion (57%) of which were followed by oscillatory $[Ca^{2+}]_i$ or $[Ca^{2+}]_i$ spikes at the frequency of 0.37 ± 0.081 tones/min with an amplitude of 163.9 ± 22.7 nM (n = 7) (Fig. 4B-b). The other 74% of the cells showed no initial response (Fig. 4B-c), but 30% of them gradually developed oscillatory $[Ca^{2+}]_i$ or $[Ca^{2+}]_n$ spikes at the frequency of 0.44 ± 0.07 tones/min with an amplitude of 195.7 ± 26.5 nM (n = 5). In the absence of extracellular Ca^{2+}, no transient rise or oscillatory change of $[Ca^{2+}]_i$ or $[Ca^{2+}]_n$ was observed, suggesting that FCS induced $[Ca^{2+}]_i$ rise or $[Ca^{2+}]_i$ oscillation is solely due to transmembrane Ca^{2+} influx. After the stimulation by FCS, the spatial distribution of $[Ca^{2+}]_i$ was inhomogeneous and $[Ca^{2+}]_i$ gradient towards the nuclei was observed. The spatial distribution of $[Ca^{2+}]_n$ was also inhomogeneous and peripheral $[Ca^{2+}]_n$ rise or central $[Ca^{2+}]_n$ rise was observed.

Effect of Thapsigargin on Temporal and Spatial Changes of $[Ca^{2+}]_i$

In order to examine the role of Ca^{2+} release from internal Ca^{2+} storage sites in regulating Ca^{2+} transient, we applied thapsigargin (Tsg), which is known to cause Ca^{2+} release from internal Ca^{2+} storage sites through the inhibitory action of Ca^{2+}-ATPase. One micromolar Tsg caused gradual rise in $[Ca^{2+}]_i$ and $[Ca^{2+}]_n$ with two peaks in the presence of extracellular Ca^{2+}

Fig. 3. **A:** Temporal changes of $[Ca^{2+}]_n$ and $[Ca^{2+}]_i$ value in typical individual HUVECs stimulated by thrombin in the presence of 1 mM $CaCl_2$ (a) or 1 mM EGTA (b). **B:** Temporal changes of mean $[Ca^{2+}]_n$ and $[Ca^{2+}]_i$ value in the population of HUVECs stimulated by thrombin in the presence of 1 mM $CaCl_2$ or 1 mM EGTA. **C:** Spatial distribution of ionized free Ca^{2+} inside HUVECs before and after the stimulation by thrombin in the presence of 1 mM $CaCl_2$ or 1 mM EGTA. Fluo-3 loaded HUVECs were stimulated by 0.05 U/ml thrombin in the presence or absence of extracellular Ca^{2+}. Digital imaging of fluo-3 fluorescence was carried out every 6 s as described in Materials and Methods. The mean Ca^{2+} concentration inside the cytosol and nuclei was calculated by averaging the fluorescence intensity in each pixel inside the respective portions. Closed symbols in A and B indicate the $[Ca^{2+}]_n$ change and open symbols in A and B indicate the $[Ca^{2+}]_i$ change. Typical images before (a, d) and at 30 s (b, e) and 2 min (c, f) after stimulation by thrombin are shown. The results presented here are the typical representative of 3 different preparations. Arrow in A, B indicates the time of addition of thrombin. Arrows in C(a,d) show compartmentalization of fluo-3 into internal organelles. Bar, 50 μm.

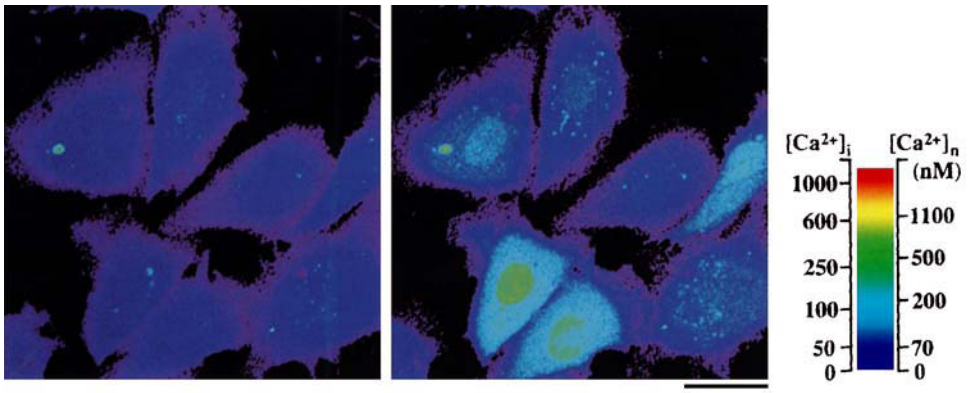

Fig. 4. **A:** Spatial distribution of $[Ca^{2+}]_i$ inside synchronized HUVECs before (a) and after (b) the stimulation by FCS in the presence of 1 mM $CaCl_2$. **B:** Temporal changes of $[Ca^{2+}]_i$ and $[Ca^{2+}]_n$ values stimulated by FCS in the presence of 1 mM $CaCl_2$. Synchronized HUVECs were prepared by culturing cells without FCS for 24 h. Synchronized HUVECs were loaded with fluo-3 as described in Materials and Methods. The cells were then stimulated by 10% FCS in the presence of extracellular Ca^{2+}. Digital imaging of fluo-3 fluorescence was carried out every 6 s as described in Materials and Methods. The $[Ca^{2+}]_i$ and $[Ca^{2+}]_n$ values were calculated by averaging the fluorescence intensity in each pixel inside the cytosol and nuclei portions. Typical images before and 30 s after the stimulation by FCS are shown in A. Three typical responses of HUVECs in the same culture to FCS are shown (B-a,b,c). Dotted lines indicate the $[Ca^{2+}]_n$ change and continuous lines indicate the $[Ca^{2+}]_i$ change. The results presented here are the typical representatives of 3 different preparations. Arrows in B indicate the time of addition of FCS. Bar, 50 μm. (Figure 4 continues on next page)

(Fig. 5A-a), while the second peak was not observed in the absence of extracellular Ca^{2+} (Fig. 5A-b) and the temporal changes of $[Ca^{2+}]_i$ and $[Ca^{2+}]_n$ were identical. As shown in Figure 5B and Table III, the mean peak $[Ca^{2+}]_i$ and $[Ca^{2+}]_n$ values at the first peak in the presence of extracellular Ca^{2+} were comparable with those in the absence of extracellular Ca^{2+}, and second $[Ca^{2+}]_i$ and $[Ca^{2+}]_n$ rise were abolished by chelating extracellular Ca^{2+}, suggesting that the main source of Ca^{2+} elevating $[Ca^{2+}]_i$ and $[Ca^{2+}]_n$ at the first spikes is the internal Ca^{2+} storage sites and transmembrane Ca^{2+} influx is necessary for the second $[Ca^{2+}]_i$ and $[Ca^{2+}]_n$ rise. The existence of $[Ca^{2+}]_i$-operated plasma membrane Ca^{2+}-channel was suggested and it may play some roles in regulating second peak of $[Ca^{2+}]_i$ and $[Ca^{2+}]_n$ rise. As shown in Figure 5C, at the first and the second peak of $[Ca^{2+}]_i$ or $[Ca^{2+}]_n$ rise, the spatial distribution of $[Ca^{2+}]_i$ or $[Ca^{2+}]_n$ in the cells was inhomogeneous in the presence or absence of extracellular Ca^{2+} as observed in the cells stimulated by thrombin. In order to investigate the relationship between Tsg sensitive internal Ca^{2+} storage sites and thrombin sensitive internal Ca^{2+} storage sites, 0.05 U/ml thrombin was applied to the HUVECs preincubated with 1 μM Tsg. Thrombin caused $[Ca^{2+}]_i$ and $[Ca^{2+}]_n$ rise in the cells preincubated with Tsg for 10 min in the presence of extracellular Ca^{2+} and no $[Ca^{2+}]_i$ and $[Ca^{2+}]_n$ rise in the absence of extracellular $[Ca^{2+}]_i$ and $[Ca^{2+}]_n$ (data not shown), suggesting that thrombin sensitive and Tsg sensitive internal Ca^{2+} storage sites should be identical, and $[Ca^{2+}]_i$ and $[Ca^{2+}]_n$ rise after the stimulation of thrombin in the cells treated with Tsg in the presence of extracellular Ca^{2+} is mainly due to extracellular Ca^{2+} influx.

DISCUSSION

In order to investigate the relationship of $[Ca^{2+}]_i$ and $[Ca^{2+}]_n$ in HUVECs, we first attempted to obtain in vivo calibration curves separately for the cytosol and the nucleus. Since several reports suggested the existence of Ca^{2+} gradients between cytosol and nucleus [Williams et al., 1985; Wahl et al., 1992; Geiger et al., 1992; Goldman et al., 1990; Tucker and Fay, 1990; Yelamarty et al., 1990; Hernandez-Cruz et al., 1990; Nakato et al., 1992; Burnier et al., 1994], Ca^{2+}-calibration in whole-cell-basis is likely to cause serious confusion in interpreting the observations. The obtained calibration curves showed that $[Ca^{2+}]_i$ and $[Ca^{2+}]_n$ were separately measurable under physiological conditions and the fluorescence intensity in the nucleus was higher than that in the cytosol, which means the higher concentration of fluo-3 inside nucleus

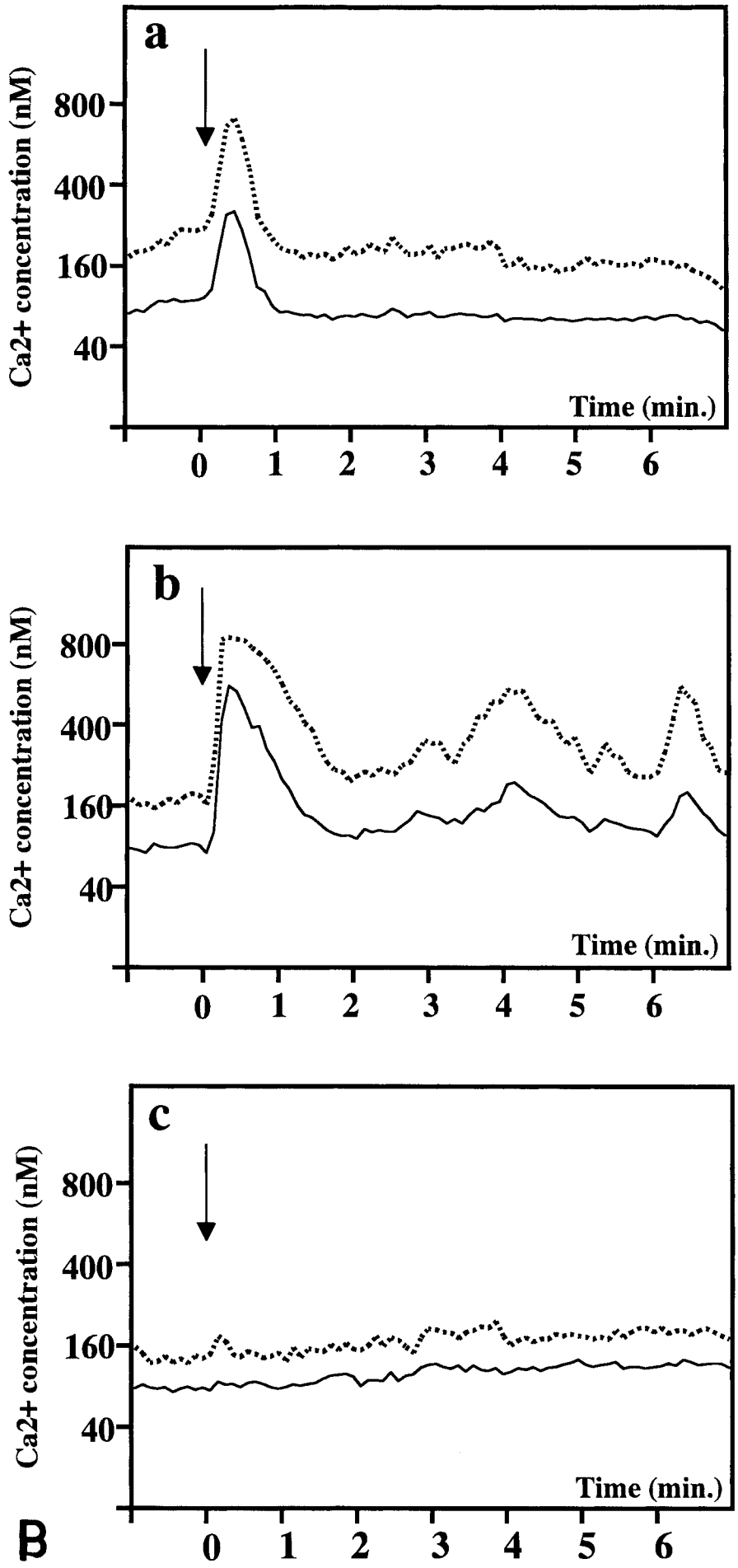

Figure 4. (Continued.)

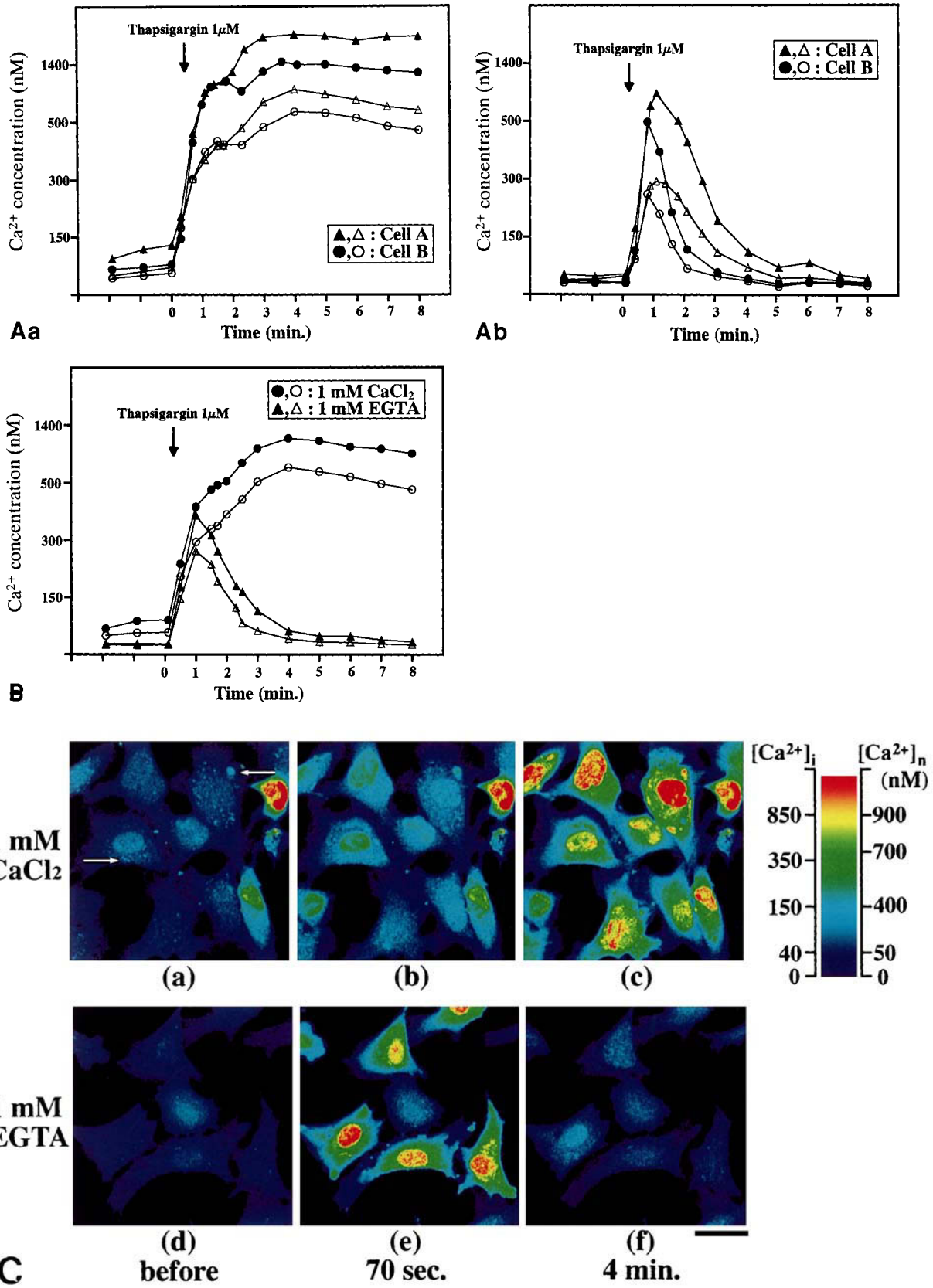
Thapsigargin 1μM
Ca2+ concentration (nM)
1400
500
300
150
▲,△ : Cell A
●,○ : Cell B
0 1 2 3 4 5 6 7 8
Time (min.)
Aa
Ab
●,○ : 1 mM CaCl2
▲,△ : 1 mM EGTA
B
1 mM CaCl2
(a)
(b)
(c)
[Ca2+]i
[Ca2+]n
(nM)
850
350
150
40
0
900
700
400
50
0
1 mM EGTA
(d) before
(e) 70 sec.
(f) 4 min.
C

Figure 5.

TABLE III. Effect of Thapsigargin (1 μM) on Changes in Cytosolic and Nuclear Calcium Concentrations in HUVECs Loaded with Fluo-3 in the Presence of 1 mM Extracellular Ca^{2+} or 1 mM EGTA†

	Cytosolic				Nuclear			
	Baseline	1st peak	2nd peak	n	Baseline	1st peak	2nd peak	n
1 mM Ca^{2+}	87.4 ± 19.7	372.6 ± 66.4*	1,031.2 ± 193.5***	26	107.2 ± 15.4	493.3 ± 80.8**	1,277.0 ± 214.4***	22
1 mM EGTA	26.3 ± 2.4	319.8 ± 55.8*		34	42.2 ± 4.6	454.5 ± 61.7*		16

†Thapsigargin was added 5 min after the addition of EGTA into the extracellular medium. Values are expressed as means ± sem in nM.
*$P < 0.0001$ vs. baseline.
**$P = 0.0002$ vs. baseline.
***$P < 0.01$ vs. 1st peak.

than cytosol. Therefore, the separate calibration of $[Ca^{2+}]_i$ and $[Ca^{2+}]_n$ is crucial to discuss the relationship of $[Ca^{2+}]_i$ and $[Ca^{2+}]_n$. Under our assay conditions, the calibrated $[Ca^{2+}]_n$ was higher than the calibrated $[Ca^{2+}]_i$ before and after stimulation, consistent with the results obtained by Geiger et al. [1992] with ECs, Williams et al. [1985] with smooth muscle cells, however inconsistent with the results by Wahl et al. [1992] with fibroblasts and Burnier et al. [1994] with smooth muscle cells and ECs, who reported lower Ca^{2+} concentration in nucleus than in cytosol. However, the mechanisms controlling $[Ca^{2+}]_n$ may vary in different cell types; this difference may be due to the differences in dye characteristics or in the calibration methods. Geiger et al. [1992] used in vitro calibration curve to measure $[Ca^{2+}]_i$ and Williams et al. [1985] and Wahl et al. [1992] used ionomycin and hypotonic buffer to obtain in vivo calibration curve for fura-2, respectively. Burnier et al. [1994] used nonfluorescent Ca^{2+} ionophore, 4-bromo-A23187 to calibrate $[Ca^{2+}]_i$ and $[Ca^{2+}]_n$ with using fluo-3 and a CLSM. The existence of Ca^{2+} gradients between cytosol and nucleus may suggest the existence of an active Ca^{2+} accumulation system on nuclear membrane even before stimulation in HUVECs, like the nuclear membrane Ca^{2+}-ATPase system reported by Kulikova et al. [1982] in skeletal muscles cells, because the Ca^{2+} gradients should be diminished if the gradients are regulated only by simple diffusion of Ca^{2+} between cytosol and nucleus. The higher concentration of ionized Ca^{2+} inside nucleus may have important roles in nucleus-specific cellular responses, like cell proliferation.

Consistent with previous reports [Goligotsky et al., 1989; Hallam et al., 1988; Lerner, 1994; Garcia, 1992; Wickham et al., 1988], we could demonstrate the initial and sustained rise of $[Ca^{2+}]_i$ induced by thrombin; the former is Ca^{2+} mobilization from internal Ca^{2+} storage sites and the latter is extracellular Ca^{2+} influx. The spatial distribution of $[Ca^{2+}]_i$ in cytosol stimulated by thrombin was inhomogeneous and $[Ca^{2+}]_i$ gradient towards the nucleus was observed at the initial $[Ca^{2+}]_i$ spike and during sustained phase in the presence of extracellular Ca^{2+}. This $[Ca^{2+}]_i$ gradient is not produced by the cell thickness, because the focal depth of our CLSM is about 0.6 μm which is sufficiently small to obtain fluorescence intensity independently of the cell thickness. This $[Ca^{2+}]_i$ gradient may therefore be produced by the Ca^{2+} mobilization from internal storage sites such as endoplasmic reticulum or mitochondria which mainly exists around the nucleus [Johnson et al., 1980; Terasaki et al., 1984]. We could not detect the Ca^{2+} influx because of the limited temporal resolution of this system or of the weak signal from the thin peripheral zones of

Fig. 5. A: Temporal changes of $[Ca^{2+}]_n$ and $[Ca^{2+}]_i$ in typical individual HUVECs stimulated by thapsigargin in the presence of 1 mM $CaCl_2$ (a) or 1 mM EGTA (b). B: Temporal changes of mean $[Ca^{2+}]_n$ and $[Ca^{2+}]_i$ value in the population of HUVECs stimulated by thapsigargin in the presence of 1 mM $CaCl_2$ or 1 mM EGTA. C: Spatial distribution of ionized free Ca^{2+} inside HUVECs before and after the stimulation by thapsigargin in the presence of 1 mM $CaCl_2$ or 1 mM EGTA. Fluo-3 loaded HUVECs were stimulated by 1 μM thapsigargin in the presence or absence of extracellular Ca^{2+}. Digital imaging of fluo-3 fluorescence was carried out every 6 s as described in Materials and Methods. The mean Ca^{2+} concentration inside the cytosol and nuclei portions was calculated by averaging the fluorescence intensity in each pixel inside the respective portions. Typical images before (a, d) and at 70 s (b, e) and 4 min (c, f) after the stimulation by thapsigargin are shown. The results presented here are the typical representatives of 3 different preparations. Arrows in A and B indicate the time of addition of thapsigargin. Arrows in C(a) show compartmentalization of fluo-3 into internal organelles. Bar, 50 μm.

the cytosol for obtaining reliable fluorescence intensity [Goldman et al., 1990].

We observed that the temporal change in $[Ca^{2+}]_n$ was identical to that in $[Ca^{2+}]_i$ induced by thrombin and Tsg, and the spatial analysis of $[Ca^{2+}]_n$ revealed that the spatial distribution of $[Ca^{2+}]_n$ was inhomogeneous and peripheral $[Ca^{2+}]_n$ rise or central $[Ca^{2+}]_n$ rise was observed during these stimulations. As the initial $[Ca^{2+}]_i$ spike induced by thrombin is due to the Ca^{2+} mobilization from internal Ca^{2+} storage sites through IP_3 generation [Goligotsky et al., 1989], it is likely that the initial $[Ca^{2+}]_n$ spike was generated by IP_3, because IP_3 receptors were found in rat liver nuclei and Ca^{2+} release from the nucleus was shown [Malviya et al., 1990; Matter et al., 1993]. The inhomogeneous Ca^{2+} distribution in the nucleus may suggest the existence of Ca^{2+} storage sites in the nuclear membrane or in the nucleus. From these results, the existence of a $[Ca^{2+}]_n$ regulating system through the action of IP_3 was suggested. However, whether the Ca^{2+} accumulation system on nuclear membrane at rest is still active after stimulation is not known and further investigation is necessary to offer a precise mechanism.

The $[Ca^{2+}]_i$ response of HUVECs to thrombin and FCS was quite heterogeneous from cell to cell, consistent with the observations in human fibroblasts stimulated by bradykinin or thrombin [Byton and Villereal, 1989], in A431 human epidermal carcinoma cells stimulated by EGF and FCS [Gonzalez et al., 1988], and in antigen stimulated rat basophilic leukemia cells [Millard et al., 1988]. Although Millard et al. presumed that heterogeneity in cellular responses may be due to receptor density, stage of cell growth or generation of second messengers such as IP_3 [Millard et al., 1988], our observed heterogeneity was not related to the cell cycle, because similar heterogeneity was also observed in synchronized cells. The relatively less heterogeneity in the response of HUVECs stimulated by Tsg suggested the heterogeneity in thrombin or FCS stimulated HUVECs may be due to heterogeneity in receptor-ligand coupling as Byron and Villereal suggested [1989]. Heterogeneity may have some important roles to maintain vascular homeostasis.

In certain parts of FCS-treated cells, we observed $[Ca^{2+}]_i$ and $[Ca^{2+}]_n$ spikes or oscillations of $[Ca^{2+}]_i$ and $[Ca^{2+}]_n$, which were completely abolished by chelation of extracellular Ca^{2+}, suggesting that FCS-induced $[Ca^{2+}]_i$ and $[Ca^{2+}]_n$ spikes are solely due to transmembrane Ca^{2+} influx independent of Ca^{2+} mobilization. These results were inconsistent with the observations in other cell types; several groups have shown that FCS-induced $[Ca^{2+}]_i$ rise is mainly due to Ca^{2+} discharge from internal Ca^{2+} storage sites in human fibroblasts [Moolenaar et al., 1984], A431 epidermal carcinoma cells [Gonzalez et al., 1988], and all retinal pigment epithelial cells [Kuriyama et al., 1991]. It is likely that the $[Ca^{2+}]_i$ controlling system may vary in each cell type. We hypothesize that transmembrane Ca^{2+} influx plays major roles in producing $[Ca^{2+}]_i$ oscillations independently of IP_3-dependent Ca^{2+} release in endothelial cells. This hypothesis is supported by the observation that $[Ca^{2+}]_i$ oscillations in bovine endothelial cells induced by bradykinin are abolished by chelating extracellular Ca^{2+} [Laskey et al., 1992].

In conclusion, we could demonstrated that $[Ca^{2+}]_n$ is constantly higher than $[Ca^{2+}]_i$ at rest or after stimulation and inhomogeneous $[Ca^{2+}]_i$ or $[Ca^{2+}]_n$ distribution after stimulation in HUVECs by employing a digital imaging CLSM system with fluo-3 and three kinds of $[Ca^{2+}]_n$ regulating systems were suggested: the first is the active Ca^{2+} accumulation system on nuclear membrane at rest, the second is the IP_3 dependent $[Ca^{2+}]_n$ regulatory system, the third is the $[Ca^{2+}]_n$ regulatory system requiring extracellular Ca^{2+} after the stimulation of FCS. We also demonstrated the heterogeneity in the $[Ca^{2+}]_i$ response of HUVECs to thrombin or to FCS. Although the physiological roles of Ca^{2+} gradients between cytosol and nucleus, localized $[Ca^{2+}]_i$ gradients and $[Ca^{2+}]_i$ oscillations, are still unclear, it is likely that a $[Ca^{2+}]_n$ or $[Ca^{2+}]_i$ rise may regulate cellular functions in a localized or repetitive fashion. Analysis using digital imaging systems may provide further insight into $[Ca^{2+}]_n$ and $[Ca^{2+}]_i$ regulating systems and $[Ca^{2+}]_n$- or $[Ca^{2+}]_i$-dependent cellular functions in single living cells.

ACKNOWLEDGMENTS

We thank Dr. Kei-ichirou Suzuki (Department of Biochemistry, Osaka University Medical School) for the donation of HUVECs and the technical advice for the collection HUVECs from umbilical cord.

REFERENCES

Buga GM, Gold ME, Fukuto JM, Ignarro LJ (1991): Shear stress-induced release of nitric oxide from endothelial cells grown on beads. Hypertension 17:187–193.

Burgoyne RD, Cheek TR, Morgan A, O'Sullivan AJ, Moreton RB, Berridge MJ, Mata AM, Colyer J, Lee AG, East JM (1989): Distribution of two distinct Ca^{2+}-ATPase-like proteins and their relationship to the agonist-sensitive calcium store in adrenal chromaffin cells. Nature 342: 72–74.

Burnier M, Centeno G, Burki E, Brunner HR (1994): Confocal microscopy to analyze cytosolic and nuclear calcium in cultured vascular cells. Am J Physiol 266:C1118–C1127.

Byton KL, Villereal ML (1989): Mitogen-induced $[Ca^{2+}]_i$ changes in individual human fibroblasts. J Biol Chem 264:18234–18239.

Garcia JGN (1992): Molecular mechanisms of thrombin-induced human and bovine endothelial cell activation. J Lab Clin Med 120:513–519.

Geiger RV, Berk BC, Alexander RW, Nerem RM (1992): Flow-induced calcium transients in single endothelial cells: Spatial and temporal analysis. Am J Physiol 262:C1411–C1417.

Gericke M, Oike M, Droogmans G, Nilius B (1994): Inhibition of capacitative Ca^{2+} entry by a Cl^- channel blocker in human endothelial cells. Eur J Pharmacol 269:381–384.

Gertler JP, Perry L, L'Italien G, Chung-Welch N, Cambria RP, Orkin R, Abbott WM (1993): Ambient oxygen tension modulates endothelial fibrinolysis. J Vasc Surg 18:939–946.

Gillo B, Ma Y-S, Marks AR (1993): Calcium influx in induced differentiation of murine erythroleukemia cells. Blood 81:783–792.

Goldman WF, Bova S, Blaustein MP (1990): Measurement of intracellular Ca^{2+} in cultured arterial smooth muscle cells using Fura-2 and digital imaging microscopy. Cell Calcium 11:221–231.

Goligotsky MS, Menton DN, Laslo A, Lum H (1989): Nature of thrombin-induced sustained increase in cytosolic calcium concentration in cultured endothelial cells. J Biol Chem 264:16771–16775.

Gonzalez FA, Gross DJ, Heppel LA, Webb WW (1988): Studies on the increase in cytosolic free calcium induced by epidermal growth factor, serum, and nucleotides in individual A431 cells. J Cell Physiol 135:269–276.

Hallam TJ, Pearson JD, Needham A (1988): Thrombin-stimulated elevation of human endothelial-cell cytoplasmic free calcium concentration causes prostacyclin production. Biochem J 251:243–249.

Haller H, Rieger M, Lindschau C, Kuhlmann M, Philipp S, Luft FC (1994): LDL increases $[Ca^{++}]_i$ in human endothelial cells and augments thrombin-induced cell signaling. J Lab Clin Med 124:708–714.

Harafuji H, Ogawa Y (1980): Re-examination of the apparent binding constant of ethylene glycol bis(β-aminoethyl ether) *N,N,N',N'*-tetraacetic acid with calcium around neutral pH. J Biochem 87:1305–1312.

Hernandez-Cruz A, Sala F, Adams PR (1990): Subcellular calcium transients visualized by confocal microscopy in a voltage-clamped vertebrate neuron. Science 247:858–862.

Himmel HM, Whorton AR, Strauss HC (1993): Intracellular calcium, currents, and stimulus-response coupling in endothelial cells. Hypertension 21:112–127.

Jaffe EA, Nachman RL, Becker CG, Minick CR (1973): Culture of human endothelial cells derived from umbilical veins. J Clin Invest 52:2745–2756.

Johnson LV, Walsh ML, Chen LB (1980): Localization of mitochondria in living cells with rhodamine 123. Proc Natl Acad Sci USA 77:990–994.

Kao JPH, Harootunian AT, Tsien RY (1989): Photochemically generated cytosolic calcium pulses and their detection by fluo-3. J Biol Chem 264:8179–8184.

Kuba K, Hua S, Nohmi M (1991): Spatial and dynamic changes in intracellular Ca^{2+} measured by confocal laser-scanning microscopy in bullfrog sympathetic ganglion cells. Neurosci Res 10:245–259.

Kulikova OG, Savost'yanov GA, Belyavtseva LM, Razumovskaya NI (1982): Investigation of the ATPase activity and ATP-dependent accumulation of Ca^{2+} by the nuclei of skeletal muscles. Effects of denervation and electrical stimulation. Biochemistry (a translation of Biokhimiya) 47:1024–1029.

Kuriyama S, Ohuchi T, Yoshimura N, Honda Y (1991): Growth factor-induced cytosolic calcium ion transients in cultured human retinal pigment epithelial cells. Invest Ophthalmol Vis Sci 32:2882–2890.

Laposata M, Dovnarsky DK, Shin HS (1983): Thrombin-induced gap formation in confluent endothelial cell monolayers in vitro. Blood 62:549–556.

Laskey RE, Adams DJ, Cannel M, van Breemen C (1992): Calcium entry-dependent oscillations of cytoplasmic calcium concentration in cultured endothelial cell monolayers. Proc Natl Acad Sci USA 89:1690–1694.

Lerner R (1994): Changes of cytosolic calcium ion concentrations in human endothelial cells in response to thrombin, platelet-activating factor, and leukotriene B4. J Lab Clin Med 124:723–729.

Lytton J, Westlin M, Hanley MR (1991): Thapsigargin inhibits the sarcoplasmic or endoplasmic reticulum Ca-ATPase family of calcium pumps. J Biol Chem 266:17067–17071.

Malviya AN, Rogue P, Vincendon G (1990): Stereospecific inositol 1,4,5-[^{32}P]triphosphate binding to isolated rat liver nuclei: Evidence for inositol triphosphate receptor-mediated calcium release from the nucleus. Proc Natl Acad Sci USA 87:9270–9274.

Matter N, Ritz MF, Freyermuth S, Rogue P, Malviya AN (1993): Stimulation of nuclear protein kinase C leads to phosphorylation of nuclear inositol 1,4,5-triphosphate receptor and accelerated calcium release by inositol 1,4,5-triphosphate from isolated rat liver nuclei. J Biol Chem 268:732–736.

Millard PJ, Gross D, Webb WW, Fewtrell C (1988): Imaging asynchronous changes in intracellular Ca^{2+} in individual stimulated tumor mast cell. Proc Natl Acad Sci USA 85:1854–1858.

Minta A, Kao JP, Tsien RY (1989): Fluorescent indicators for cytosolic calcium based on rhodamine and fluorescein chromophores. J Biol Chem 264:8171–8178.

Moolenaar WH, Tertoolen LGJ, de Laat SW (1984): Growth factors immediately raise cytoplasmic free Ca^{2+} in human fibroblasts. J Biol Chem 259:8066–8069.

Moore ED, Becker PL, Fogarty KE, Williams DA, Fay FS (1990): Ca^{2+} imaging in single living cells: Theoretical and practical issues. Cell Calcium 11:157–179.

Nakato K, Furuno T, Inagaki K, Teshima R, Terao T, Nakanishi M (1992): Cytosolic and intranuclear calcium signals in rat basophilic leukemia cells as revealed by a confocal fluorescent microscope. Eur J Biochem 209:745–749.

Nicotera P, McConkey DJ, Jones DP, Orrenius S (1989): ATP stimulates Ca^{2+} uptake and increases the free Ca^{2+} concentration in isolated rat liver nuclei. Proc Natl Acad Sci USA 86:453–457.

Nicotera P, Bellomo G, Orrenius S (1990): The role of Ca^{2+} in cell killing. Chem Res Toxicol 3:484–494.

Person JD (1993): The control of production and release of haemostatic factors in the endothelial cell. Baillèire Clin Haematol 6:629–651.

Poenie M, Alderton J, Tsien RY, Steinhatdt RA (1985): Changes of free calcium levels with stages of the cell division cycle. Nature 315:147–149.

Rasmussen H (1986): The calcium messenger system. N Eng J Med 314:1094–1101, 1164–1170.

Rubanyi GM (1993): The role of endothelium in cardiovascular homeostasis and diseases. J Cardiovasc Pharmacol 22(Suppl. 4):S1–S14.

Terasaki M, Song J, Wong JR, Weiss MJ, Chen LB (1984): Localization of endoplasmic reticulum in living and glutaraldehyde-fixed cells with fluorescent dyes. Cell 38:101–108.

Thastrup O, Cullen PJ, Drøbak BK, Hanley MR, Dawson AP (1990): Thapsigargin, a tumor promoter, discharges intracellular Ca^{2+} stores by specific inhibition of the endoplasmic reticulum Ca^{2+}-ATPase. Proc Natl Acad Sci USA 87:2466–2470.

Tucker RW, Fay FS (1990): Distribution of intracellular free calcium in quiescent BALB/c 3T3 cells stimulated by platelet-derived growth factor. Eur J Biol 51:120–127.

Wahl M, Lucherini MJ, Gruenstein E (1990): Intracellular Ca^{2+} measurement with Indo-1 in substrate-attached cells: Advantages and special considerations. Cell Calcium 11: 487–500.

Wahl M, Sleight RG, Gruenstein E (1992): Association of cytoplasmic free Ca^{2+} gradients with subcellular organelles. J Cell Physiol 150:593–609.

Wickham NWR, Vercellotti GM, Moldow CF, Visser MR, Jacob HS (1988): Measurement of intracellular calcium concentration in intact monolayers of human endothelial cells. J Lab Clin Med 112:157–167.

Williams DA, Fogarty KE, Tsien RY, Fay FS (1985): Calcium gradients in single smooth muscle cells revealed by the digital imaging microscope using Fura-2. Nature 318: 558–561.

Yelamarty R, Miller BA, Scaduto RC, Yu FTS, Tillotson DL, Cheung JY (1990): Three-dimensional intracellular calcium gradients in single human burst-forming units-erythroid-derived erythroblasts induced by erythropoietin. J Clin Invest 85:1799–1809.